Static Cyclic Load Tests on Model Foundations in Dry Sand

Y.S. Unsever[1], T. Matsumoto[2], S. Shimono[2] and M.Y. Özkan[1]
[1]*Department of Civil Engineering, Middle East Technical University, Ankara, Turkey*
[2]*Graduate School of Natural Science and Technology, Kanazawa University, Kanazawa, Japan*
E-mail: unsever@metu.edu.tr
E-mail: matsumoto@se.kanazawa-u.ac.jp
E-mail: shimono@se.kanazawa-u.ac.jp
E-mail: myozkan@metu.edu.tr

ABSTRACT: The behaviour of pile foundations under horizontal loading was investigated by static cyclic horizontal load tests on model pile foundations including single pile, capped pile (single pile with a small raft), 3-pile pile group, 3-pile piled raft and raft alone in dry model ground. In order to consider the dead load of the superstructure, vertical load was applied to the foundations before applying horizontal load. Vertical load tests on the model foundations were also carried out to understand and discuss the behaviour of the model foundations subjected to horizontal loading. The raft effect, the effect of vertical load and their influence on the behaviour of the model foundations were investigated. The piles were instrumented with strain gauges to measure bending moments, shear forces and axial forces. The results showed that the piled raft model settles only a half of the pile group, whereas the tilting of the raft for both model types is similar under same horizontal loading. Also, the maximum bending moment and its location along the piles differ according to the foundation type.

1. INTRODUCTION

If the soil strength beneath a superstructure is not sufficient to carry the loads from the structure, the depth of foundation is increased to transfer the loads to stronger soil layers by using pile foundations. In Turkey and Japan, pile foundations are used widely, and these foundations may be subjected to horizontal loading such as earthquakes, winds, etc. in its lifetime. Number of studies on horizontal loading of pile foundations were reported, e.g. Shibata et al. (1989), Murono et al. (1997), Tokimatsu et al. (2004), Tokimatsu et al. (2005), Ishizaki et al. (2012). Behaviour of model pile foundations in dry or saturated grounds subjected to static or dynamic (seismic) loading were investigated in these research works. In which, the bottoms of the model piles are fixed to the bottom of the soil containers so that the piles are essentially end-bearing piles such as rock-socketed piles. In most of the cases, horizontal deformations of the foundations subjected to horizontal loading are investigated.

Applications of piled raft foundations to buildings are increasing in Japan and field monitoring of piled raft foundations were carried out, e.g. Yamashita et al. (2011) and Yamashita (2012). The field monitoring data show that the pile raft foundations are stable even against severe earthquakes. In these piled raft foundations, pile lengths are relatively large and they are essentially end-bearing where the piles are sat on sufficiently firm bearing strata.

In order to widen the application of piled raft, behaviour of piled rafts supported by friction piles needs to be understood and a pertinent design approach needs to be established. Centrifuge modelling of piled rafts in dry sand subjected to static and dynamic horizontal loads were carried out by Horikoshi et al. (2003a, 2003b). Similar experiments were carried out by Matsumoto et al. (2004a, 2004b, 2010) at 1-g field. The results of these experimental studies show that piled raft foundation is stable compared to pile groups when subjected to static or dynamic horizontal loading.

A series of load tests which included static and dynamic loading of different model foundations, such as single pile, capped pile, pile group, raft alone and piled raft, were carried out in this research to investigate behaviour of piled rafts in dry and saturated sand in more detail.

In this paper, a part of the test series is presented focusing on vertical and cyclic horizontal load tests of various foundation types in dry sand.

2. TEST DESCRIPTION

2.1 Model Ground and Model Foundations

Figure 1 shows the schematic illustration of the piled raft model under the loads. Silica sand #6 was used as a model ground. The physical properties of the sand are summarised in Table 1. The internal friction angle was estimated from direct shear tests.

Model ground having a relative density, D_r, of about 70 % was prepared in a laminar box that had dimensions of 800 mm (in *x*-direction) x 500 mm (in *y*-direction) with a depth of 530 mm (Figure 1).

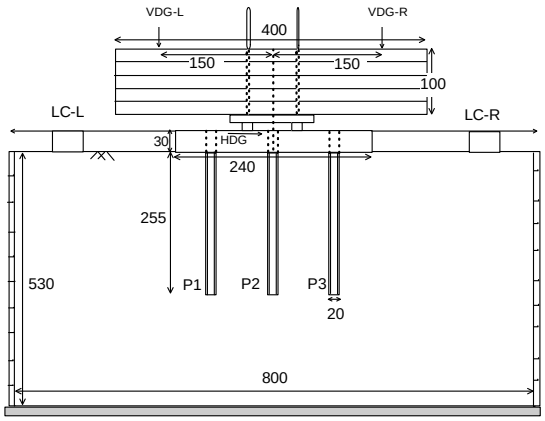

Figure 1 Test setup for piled raft

Table 1 Properties of model ground

Item	Value
Density of soil particles, ρ_s (t/m^3)	2.66
Maximum dry density, ρ_{dmax} (t/m^3)	1.542
Minimum dry density, ρ_{dmin} (t/m^3)	1.280
Maximum void ratio, e_{max}	1.079
Minimum void ratio, e_{min}	0.725
Median grain size, D_{50}	0.423
Coefficient of uniformity, U_c	1.880
Internal friction angle, ϕ' (deg)	36

Same soil container and ground conditions were used for all tests. The container consists of 10 rings each having a height of 50 mm (Figure 1).

Figure 2 shows the single model pile, made of aluminium hollow tubes and the properties of which are summarised in Table 2. The total length of the pile was 285 mm, where the upper 30 mm was embedded in the raft in case of piled raft (PR) or pile group (PG) model, resulting in the effective length of 255 mm. Tip of the pile was closed with pile cap which had a thickness of 5 mm. The pile was instrumented with strain gauges at a total of 6 levels to obtain axial forces, bending moments and shear forces induced in the pile during loading tests. Note that, after sticking strain gauges, the pile was covered with the silica sand particles to protect the strain gauges and also to obtain frictional surface between the pile and the model ground.

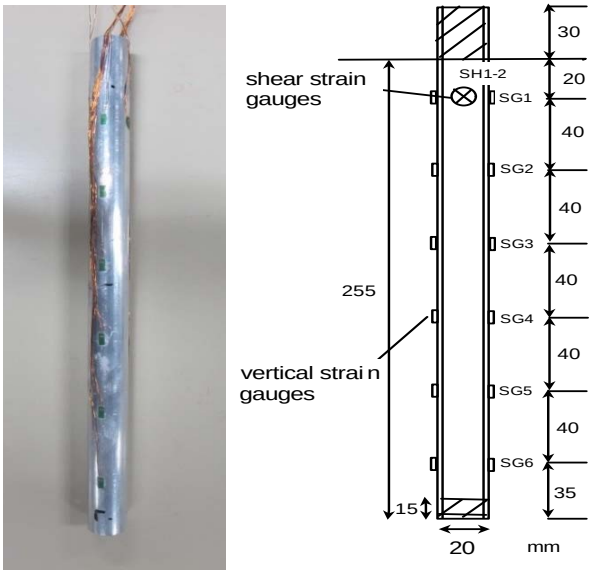

Figure 2 Model pile

Table 2 Properties of the model pile

Outer diameter, D (mm)	20.00
Wall thickness, t (mm)	1.1
Length, L (mm)	255
Cross sectional area, A (mm^2)	65.31
2nd moment of area, I (mm^4)	2926.2
Young's modulus, E (N/mm^2)	64000
Poisson's ratio, υ	0.31

Piled raft (PR) or pile group (PG) model was composed of three model piles and a rectangular raft of stainless steel having dimensions of 240 x 80 mm with a thickness of 30 mm (Figure 3).

The bottom of the raft was covered with the silica sand particles to obtain frictional surface between the raft and the ground during horizontal loading. Centre-to-centre pile spacing, s, was 80 mm, 4 times the pile diameter, D = 20 mm (s/D = 4). Pile spacing ratio s/D of 2.5 to 3 is usually adopted in conventional design of pile group. In contrast in design concept of piled raft, it is intended that the raft carries a portion of the applied vertical load by reducing the number of piles or the pile length. Hence, a pile spacing ratio s/D = 4 was selected in this particular study. The same model foundation was used for both cases of PR and PG, however 20 mm space was provided between the raft and the model ground surface for pile group (PG) case. Capped pile (CP) was composed of one model pile and a small square raft having a width of 80 mm with a thickness of 30 mm. Rafts of PR and CP were also used without piles as a full raft (FR) and small raft (SR) to evaluate the raft alone behaviour, respectively.

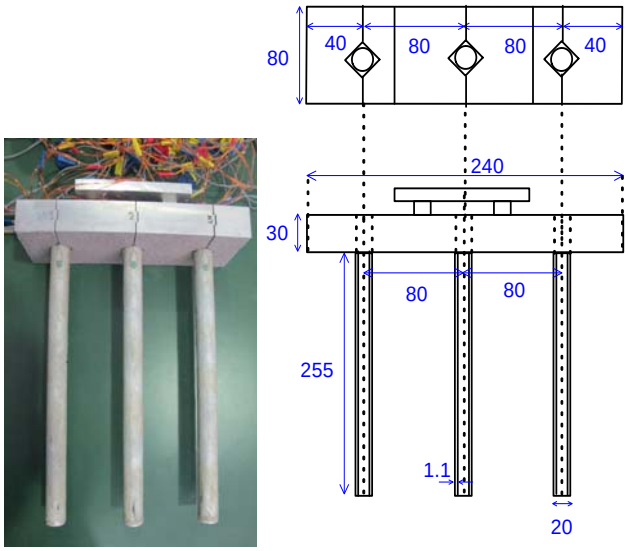

Figure 3 Piled raft (or pile group) model

2.2 Similitude for Model Tests at 1-g Gravitational Field

It is important to satisfy similitude principles to deduce the behaviour of a prototype from the behaviour of the scaled model. Iai (1989) proposed conditions for similitude for 1-g model tests, which is briefly reviewed below. Let λ be the geometrical scaling factor (prototype size / model size). Then, the scaling factor for stress, λ_σ, is given by the following relation where the same soil as the prototype soil is used for the model ground, since the gravitational accelerations in the prototype and the model are the same at 1 g:

$$\sigma_p / \sigma_m = \lambda_\sigma = \lambda \tag{1}$$

where σ is the stress in the soil and subscripts 'm' and 'p' denote 'model' and 'prototype', respectively.

For the case where the stiffness of soil at small strain level is proportional to the square root of the confining pressure, $\sqrt{\sigma}$, the scaling factor for the strain, λ_ε, is given by

$$\varepsilon_p / \varepsilon_m = \lambda_\varepsilon = \sqrt{\lambda} \tag{2}$$

The similitude for model test at 1-g field can be summarised as shown in Table 3. The similitude for 1-g field model tests is rather complex as compared with the centrifuge modelling.

Table 3 Similitude for model test at 1-g field

Item	prototype / model
Length (Size)	λ
Density	1
Stress	λ
Strain	$\lambda^{1/2}$
Shear modulus	$\lambda^{1/2}$
Time	$\lambda^{3/4}$
Frequency	$1/\lambda^{3/4}$
Displacement	$\lambda^{3/2}$
Velocity	$\lambda^{3/4}$
Acceleration	1
Bending rigidity of pile	$\lambda^{9/2}$
Longitudinal rigidity of pile	$\lambda^{5/2}$

One-dimensional compression test of the sand was conducted using an oedometer test device to obtain one-dimensional modulus (constrained modulus), E_c, of the sand. Figure 4 shows the relationship of E_c and effective vertical stress, σ'. The lines in the figure were drawn using a relation of Eq. (3).

$$E_c = E_{cref}\left(\frac{\sigma'}{\sigma_{ref}'}\right)^n \quad (3)$$

E_{cref} = constraint elastic modulus at $\sigma' = \sigma_{ref}'$
σ' = effective overburden vertical stress
σ_{ref}' = reference stress (taken as 100 kPa)
n = exponent

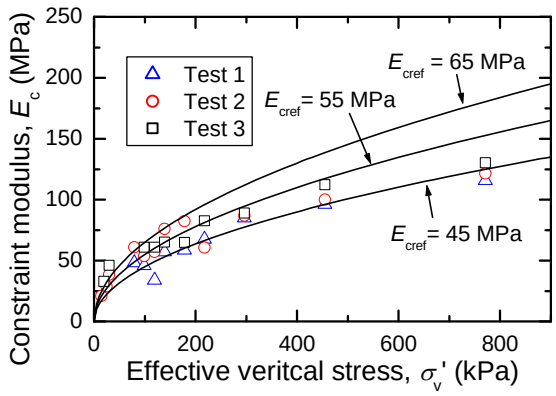

Figure 4 Relationship between the elastic constraint modulus, E_c, with effective stress, σ'

As it is roughly obtained from the figure, E_{cref} = 50 MPa and n = 0.5. That is, the stiffness of the sand is proportional to the square root of the confining pressure. Hence, the similitude rules shown in Table 3 could be applied to the model tests in this paper. In case of scale ratio of λ = 30, the bending rigidity, EI, and longitudinal rigidity, EA, of a prototype pile are 4.35 and 0.41 times those of a concrete pile ($E = 3\times10^6$ kPa) having a diameter of 0.6 m and a length of 7.65 m, which means a "short pile" condition.

Note that the test results are presented in model scale in this paper.

2.3 Test Procedure

Test procedures for vertical and horizontal loading tests are summarised as:

1) Prepare the model ground by layers (10 layers of 50 mm and one layer of 30 mm) in order to control the density of the model ground. Place (pour) 6 soil layers (which makes totally 280 mm height) one by one and compact until an intended relative density of 70 %.
2) Fix the model foundation on the box by the help of clamps and rods.
3) Place (pour) 5 more soil layers of soil until 530 mm height of the model ground was obtained.
   The piles are considered to be cast-in-place piles by adopting steps 1 to 3, because sand was poured around the piles then compacted lightly. In reality, variations of strains of the piles were very small during the preparation of the model ground. The strains of the piles were initialised (zeroed) at the end of preparation of the ground and the model foundation.
4) Set load cells and dial gauges to measure applied load and deformations.

For vertical loading:

5v) Apply the vertical load by the help of screw jack with constant displacement rate.

For horizontal loading:

5h) Place mass plates (weights) one by one on top of the raft to apply vertical load until a desired loading level was reached. Then, fix the plates to the raft by bolting.
6h) Apply horizontal load in longitudinal direction by means of rotating wooden rods and pulling wires (Figures 1 and 5).

In the first cyclic horizontal loading, the displacement was applied to the raft in the right (positive) direction until u/D reaches 0.2, then the loading direction was inverted to the left (negative) direction until u/D reaches -0.2, where u is the horizontal displacement and D is the pile diameter. In total, three cyclic loadings were applied similarly, until u/D reaches ±0.2, ±0.4 and ±0.6 in each loading cycle.

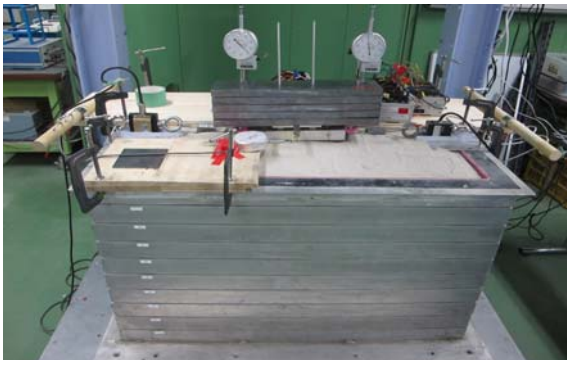

Figure 5 Photo of the experiment setup with instrumentations

3. TEST RESULTS

3.1 CPT Test Results

In order to check the uniformity of the distribution of the soil strength of the model ground and to confirm the repeatability of the tests, a miniature cone penetrometer, having a diameter of 20 mm with an apex angle of 60 degrees, was used. The measured tip resistances, q_c, on 4 different test grounds with 6 different locations for each test are summarised in Figure 6. It can be said from Figure 6 that the model grounds are almost uniform for all tests. It is also seen that q_c increases almost linearly with increasing depth. It should be noted that CPTs were carried out for a separate model ground without model foundation. It is confirmed that q_c is not influenced by the side walls if the location is far from the side walls by 50 mm.

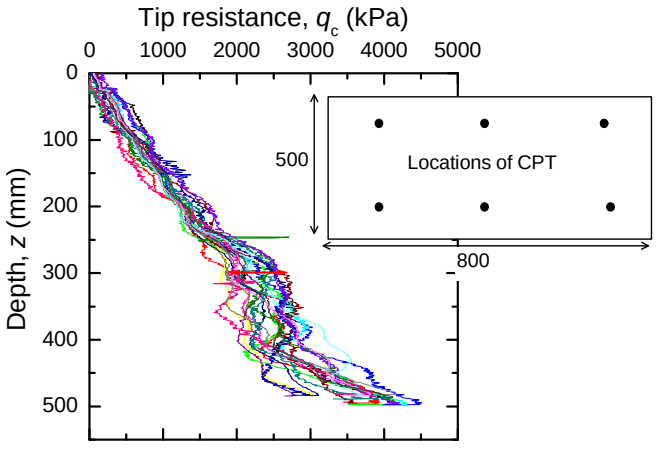

Figure 6 CPT results of model grounds in different model tests

3.2 Vertical Load Test Results

Even when a piled raft or a pile group is subjected to horizontal loading alone, compression or tension loads are induced in piles

depending upon locations of the piles in the foundation. Hence, responses of the model foundations subjected to vertical loading were investigated first. The test results would be beneficial for understanding response of the foundations subjected to horizontal loading.

Load (*V*)-settlement (*w*) relationships obtained from Single pile (SP), Capped pile (CP) and Small raft (SR) experiments are shown in Figure 7. The loads of pile and raft in CP are also indicated in this figure. These loads were obtained from the total applied load and the axial force near the pile head. Load test of SR alone was terminated at a settlement, *w*, of 10 mm, because the ultimate capacity of 800 N was obtained at a settlement of 9 mm and the raft tended to tilt after the ultimate capacity. SP and CP were loaded until the settlements reached 17.5 mm that was 88 % of the pile diameter or 22 % of the square raft width. It can be seen from the figure that the sum of the resistances of SP and SR is smaller than that of CP until the settlement of 10 mm. It is supposed that the sum of the resistances of SP and SR becomes to be almost equal to that of CP when the settlement reaches 17.5 mm. This result clearly shows the interaction of the raft and the single pile in CP. That is, response of CP cannot be obtained from the mere sum of SP and SR. In the CP experiment, the mobilised raft resistance at a given settlement was smaller than that of SR alone.

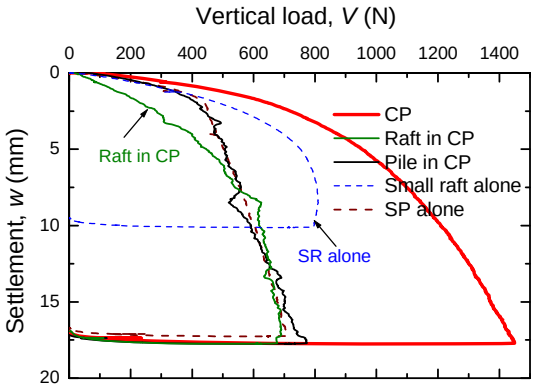

Figure 7 Loads supported by components of CP, together with loads of each component alone tests

Figure 8 shows the distributions of axial forces of the single pile (SP) and the pile in CP model at different normalised settlement, *w*/*D*. It can be seen that the axial forces of the pile in CP are a little larger than those of SP at each *w*/*D*. This may be caused by the load transfer from the raft bottom to the ground, resulting in increase in horizontal stresses on the pile shaft and stiffness of the ground surrounding the piles, as suggested by Horikoshi et al. (2003a).

Load-settlement relationships of Piled raft (PR), Full raft (FR) and three times Single pile responses (3×SP) are shown in Figure 9. The resistance of PR was larger than that of the sum of 3×SP and FR at all settlements.

Loads of the raft and the 3 piles in PR are shown in Figure 10. It is interesting that the load supported by 3 piles in PR is extremely larger than that of 3×SP and that the stiffness of the raft in PR is exceedingly larger than that of FR, exhibiting a larger influence of interaction of the piles and the raft in PR, compared to the case of CP (Figure 7). It is clear that the sum of the resistance of 3 piles in PR.is much larger than 3 times of the resistance of pile in CP.

The proportions of vertical loads carried by the 3 piles and the raft in PR model with settlement of the raft are given in Figure 11. Until a settlement of 0.8 mm (4 % of *D*), the piles support larger portion of the total vertical load. The 3 piles reach the yield state at this settlement (see Figure 10). Thereafter, the raft supports a little bit larger load than the piles. The load supported by the piles again becomes larger than that of the raft after the settlement exceeds 5 mm, and finally the piles support 60 % of the total load.

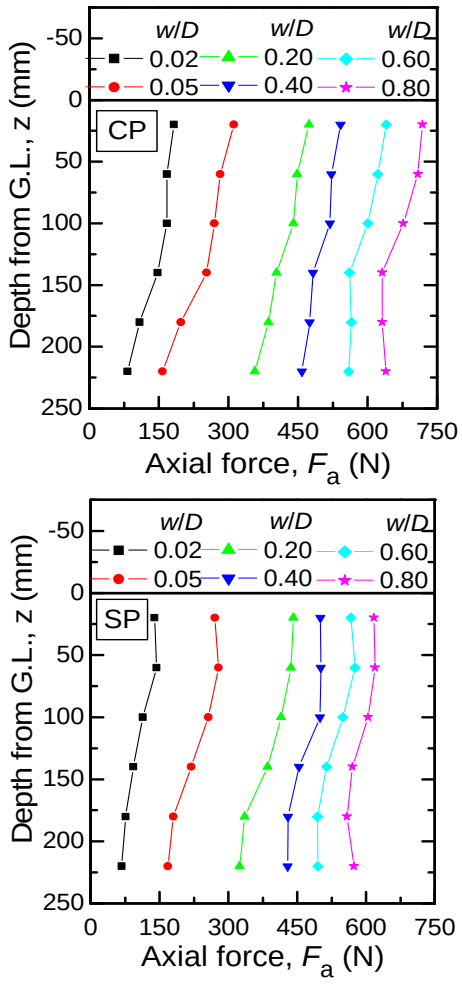

Figure 8 Axial force distribution along SP and CP models

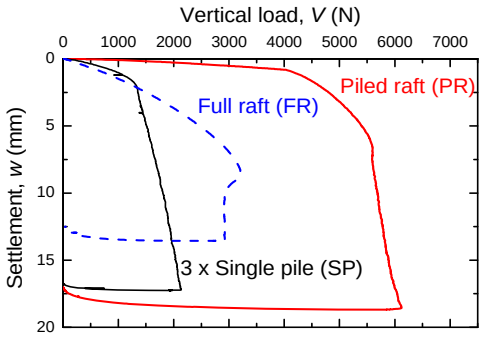

Figure 9 Comparison of PR, 3×SP and FR under vertical loading

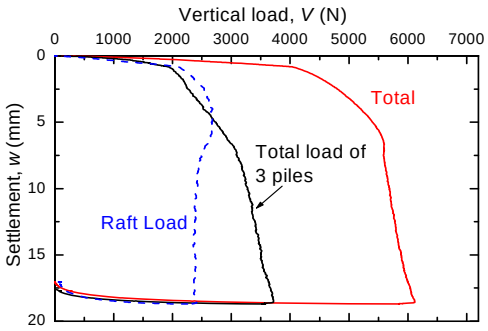

Figure 10 Sharing of vertical load between piles and raft in PR

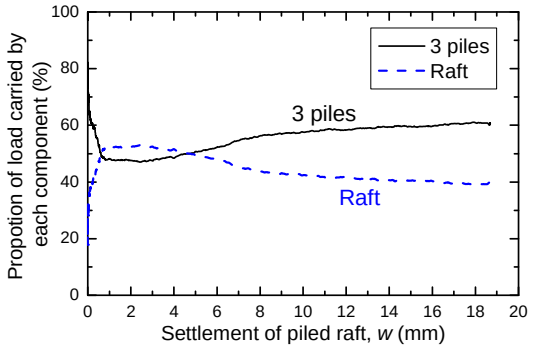

Figure 11 Proportion of vertical load carried by each component

Figure 12 shows the distributions of axial forces of 3 piles (P1, P2 and P3) in PR model at different normalised settlements. Note that P2 is the centre pile. It can be seen from comparison of Figures 8 and 12 that axial forces along the piles in PR model are larger than those of SP model. It is interesting to notice from Figure 12 that axial forces of P2 (centre pile) are larger than those of P1 and P3 (edge piles). If the ground were uniform elastic material, the edge piles support larger vertical load compared with the centre pile in case of a rigid raft because of interaction between the raft, the piles and the ground.

However, the measured results are contrast to the above mentioned situation. This is again explained by the influence of load transfer from the raft base to the ground. It is reasonable that the larger stresses are induced in the ground surrounding the centre pile (P2) compared with the ground surrounding the edge piles (P1 and P3). As the dry sand was used for the model ground in this study, rigidity and strength of the sand as well as horizontal stresses acting of the pile shaft would increase with increasing the stress level. As a result, the vertical resistance of P2 increased in this particular case of 3-pile piled raft. In case of piled rafts with a number of piles, similar phenomena might occur. However, distribution of vertical resistance of the piles would be influenced by the pile locations and the raft-soil stiffness ratio.

3.3 Horizontal Cyclic Load Test Results

3.3.1 Raft alone models (SR and FR)

The horizontal load, H vs. normalised horizontal displacement, u/D of the horizontal cyclic tests for the small raft (SR) and the full raft (FR) without vertical loading are shown in Figure 13. Note that the raft models had no pile, but the horizontal axis represents the horizontal displacement, u, normalised by the diameter, D, of the model pile for a purpose of comparison with the test results of PR and PG presented later in this paper. Self-weights of SR and FR are 7.79 N and 20.17 N, respectively.

It is seen that, the normalised horizontal displacements, where the slippage occurs, are very small, indicating that the raft base shear resistance is very effective to reduce the horizontal displacement of the raft foundation until the occurrence of slippage. Therefore, the rafts are "horizontal displacement reducers" until the slippage occurs. In addition, a series of horizontal loading tests were performed on both rafts under different vertical loads to obtain the friction angle, δ, between the contact surface and the model ground. The values of $\delta = 29.3$ deg. and 31.1 deg. were obtained for SR and FR, respectively.

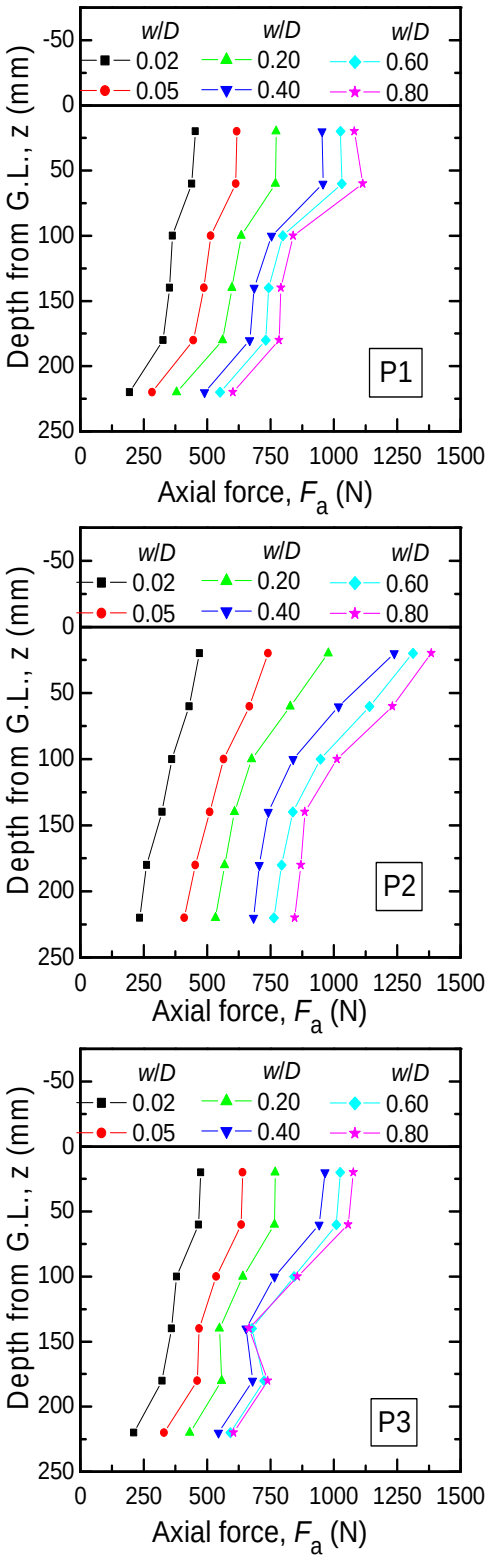

Figure 12 Axial force distributions along components of PR (P1, P2 and P3)

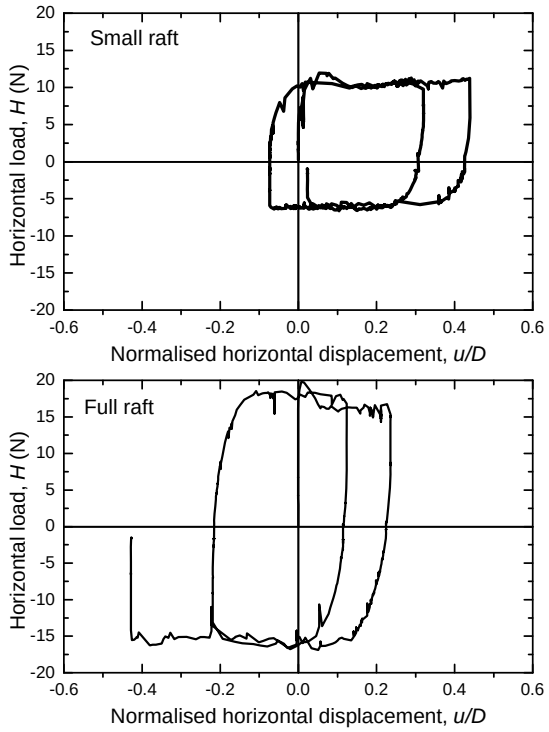

Figure 13 Horizontal load-displacement relationship of SR and FR

Variation of the initial horizontal stiffness, $k_h = (\Delta H/A)/\Delta u$, of the small raft and the full raft with the average contact pressure, $p_b = V/A$ where A is the contact area of the raft, are shown in Figure 14. It is seen from the figure that $\Delta H/\Delta u$ of both rafts tends to increase with increasing average contact pressure, p_b. This tendency may be explained by the increase in the stress levels in the ground beneath the raft, resulting in increase of the soil stiffness. If we compare the k_h values of both rafts, it is seen that k_h values of the full raft are obviously smaller than those of the small raft. The ratio of k_h of the full raft to the small raft is about 1/3. This result clearly shows the size effect on k_h since the ratio of $A_{fullraft}/A_{smallraft}$ is 3.0. In other words, $\Delta H/\Delta u$ of the full and small rafts are similar because of the size effect.

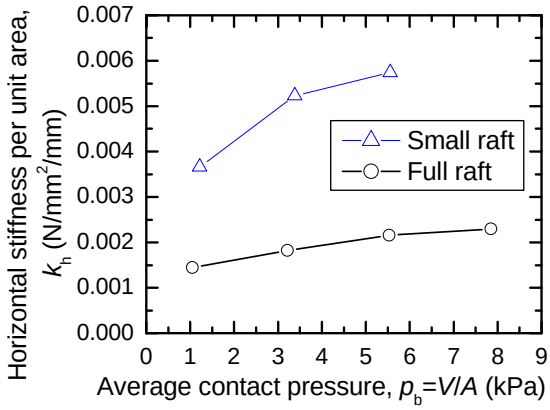

Figure 14 Horizontal stiffness per unit area k_h vs. average contact pressure p_b

3.3.2 Piled raft (PR) and pile group (PG)

In cyclic horizontal load tests of the piled raft (PR) and the pile group (PG) models, a vertical load of 496.5 N was applied on the top of the raft by placing 5 lead plates (see Figure 1) prior to the start of the horizontal loading. In the horizontal loading, as mentioned earlier, the raft was pulled to the right (positive) and left (negative) directions alternately in a displacement-controlled manner by means of wires and rotating bars. Horizontal pulling forces in both directions were measured by two load cells, and horizontal displacement and vertical displacement of the raft were measured by three dial gauges (one horizontal and two vertical) (see Figures 1 and 5). In the three cycles of horizontal loading, u/D = ±0.2, ±0.4 and ±0.6 were applied in each cycle.

The horizontal load vs. normalised horizontal displacement of the static cyclic horizontal test for the pile raft (PR) and the pile group (PG) are shown in Figure 15(a). It is clearly seen that horizontal resistance of PR is larger than that of PG for all u/D. The horizontal resistance of PG levels off at u/D = ±0.4 having a value of about 320 N. In contrast, the horizontal resistance of PR continues to increase even after u/D exceeds ±0.5.

Zoom-up of the initial loading part is shown in Figure 15(b). The horizontal stiffness of PR is much larger than that of PG, as expected from the horizontal load tests of raft alone models (Figure 13). That is, shear resistance at the raft base is effectively mobilised and suppresses the horizontal displacement in PR.

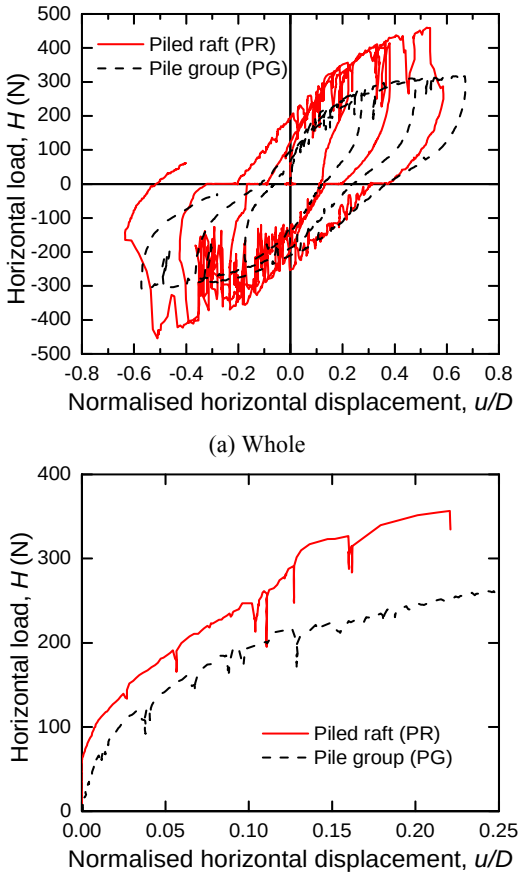

Figure 15 Horizontal load-displacement relationships of PR and PG

The horizontal load carried by each pile in PR and PG is given in Figures 16 (a) and (b). Total load is the load applied to the raft, and load of each pile is the shear force measured near pile head (20 mm below the pile head, see Figure 2). P3 is front pile and P1 is rear pile in positive loading, vice versa in negative loading. It is seen from the figures that the front pile carries most of the horizontal load and the rear pile carries least of the load for both cases. The horizontal load of centre pile P2 in positive and negative loading directions are almost equal.

It is interesting to note that the front pile in PR supports higher load compared to that in PG. This result indicates an effect of load transfer from the raft base to the ground. As the raft moved in the positive direction, the raft inclined in clock-wise direction (as shown

in Figure 17) and the settlement of the raft was larger at the position of P3. In such situation, the pile head axial force of P3 increases, although the details are not shown in the paper. Hence, load transfer from the raft base to the ground is thought be larger in the ground around P3, resulting in higher strength and stiffness of the ground. As a result, the horizontal resistance of P3 (front pile) is enhanced.

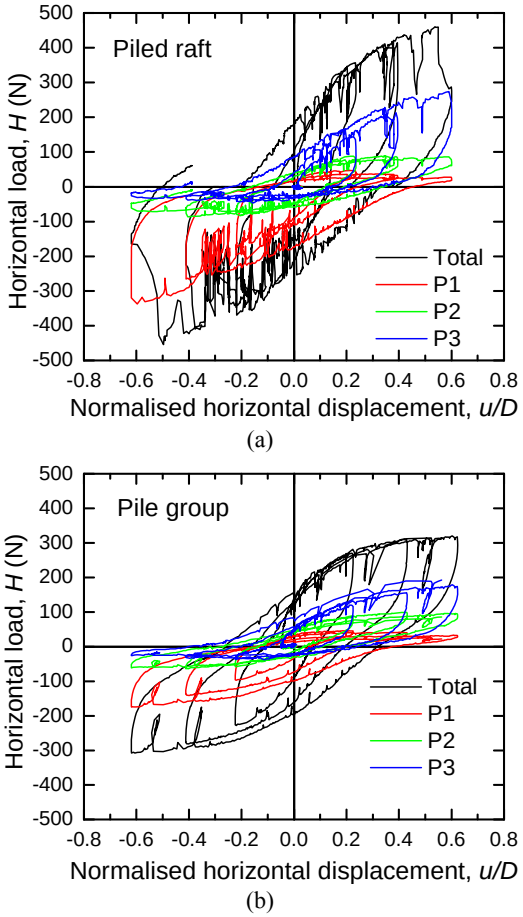

Figure 16 Horizontal load of each pile vs. normalised displacement of (a) PR and (b) PG

Inclination and vertical displacement and of the raft during the cyclic horizontal loading are shown in Figures 17 and 18, respectively. The inclination, α, of the raft is between +2 and -3 degrees in PR, +2 and -1 degrees in PG, where positive inclination means turning of the raft towards clock-wise direction (Figure 17). The inclination of the raft increases almost linearly with increasing horizontal displacement of the raft in both models. Similar result was observed also in Unsever et al. (2013).

Vertical displacements were measured at two locations (see Figure 5). The vertical displacement shown in Figure 18 is the average of two measured vertical displacements. When the raft moved horizontally, locations of the measured points on the raft also moved as the locations of the dial gauges were fixed. Hence, the average vertical displacements at $u/D = 0$ alone are correct values.

It is clearly seen from Figure 18 that the settlement of PR was suppressed compared with that of PG, indicating a favourable effect of the existence of the raft. Permanent settlement of the raft was about 10 % of the pile diameter in PR, which was a half of PG model.

The proportion of horizontal load that carried by the 3 piles during cyclic horizontal loading of PR model is shown in Figure 19. The proportion is relatively stable having a value of roughly 80 % during the cyclic loading.

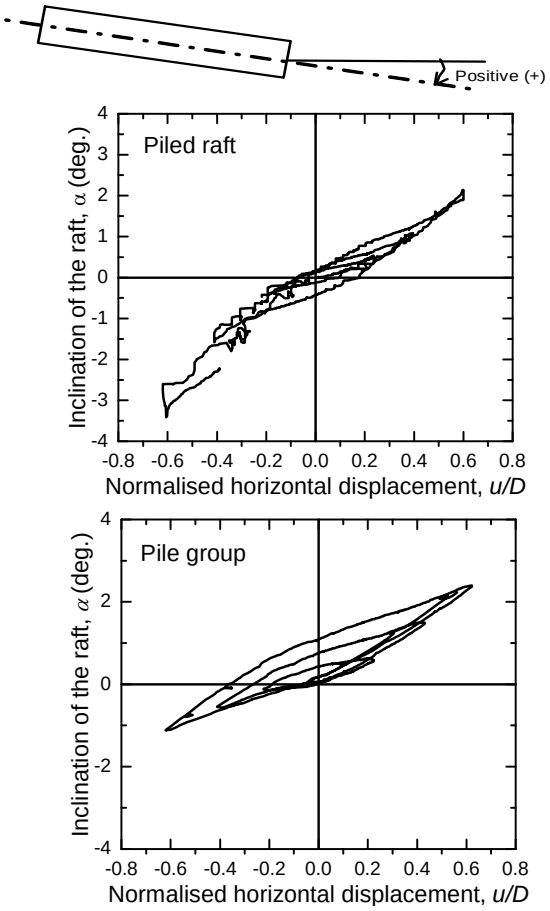

Figure 17 Inclination of the raft during cyclic horizontal loading

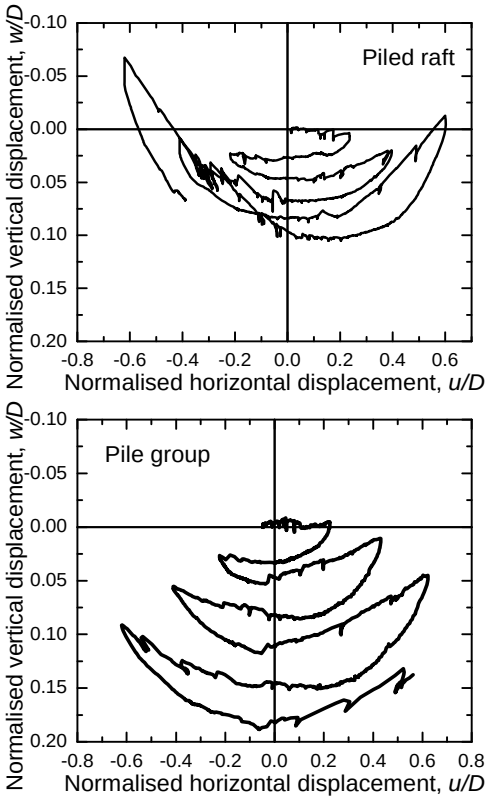

Figure 18 Vertical displacement of the raft during cyclic horizontal loading

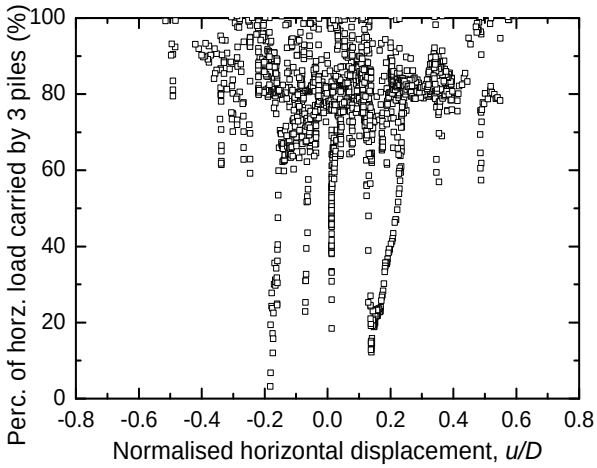

Figure 19 Percentage of horizontal load carried by 3 piles vs. normalised horizontal displacement

The proportion of vertical load that carried by the 3 piles during cyclic horizontal loading of PR model is shown in Figure 20. The proportion is again relatively stable having a value of roughly 70 % during the cyclic loading.

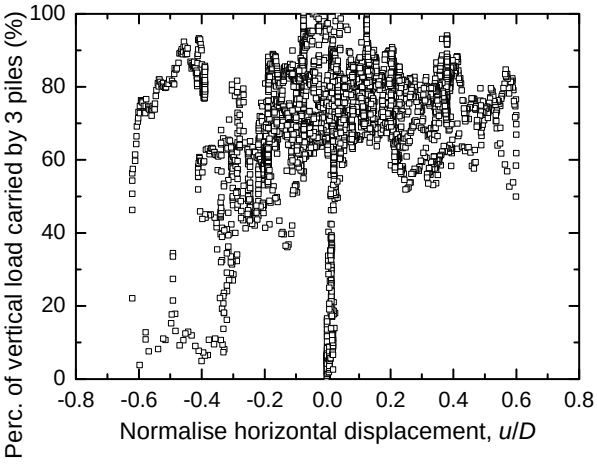

Figure 20 Percentage of vertical load carried by 3 piles vs. normalised horizontal displacement

Hereafter, response of each pile in PR and PG models are presented. In order to calculate shear forces, Q_i, and lateral soil resistance, R_{Hi}, generated on the pile section i approximately, the following equations were used:

$$Q_i = \left(M_{i+1} - M_i\right) / \mathrm{dz} \tag{4}$$

$$R_{Hi} = \left(Q_{i+1} - Q_i\right) \tag{5}$$

where M_i is the bending moment in the pile section, i and dz is the length of the pile section (Figure 21). M_i can be estimated from the measured axial strains, and the mechanical and geometrical properties of the model pile.

Changes of bending moments with u/D at different levels (see Figure 2) of each pile during horizontal loading are shown in Figures 22 and 23 for PR and PG models, respectively. Note that P3 is the front pile and P1 is the rear pile for positive loading. It is seen from the figures that the front piles carry the most of the applied horizontal load, and the rear piles carry the least in both cases. The centre piles have almost equal loads for positive and negative loading.

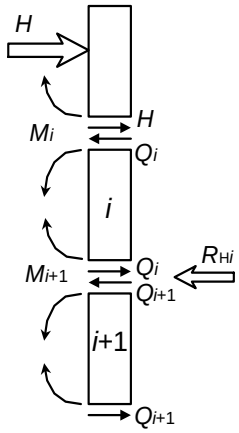

Figure 21 Approximate methods to estimate shear force and lateral

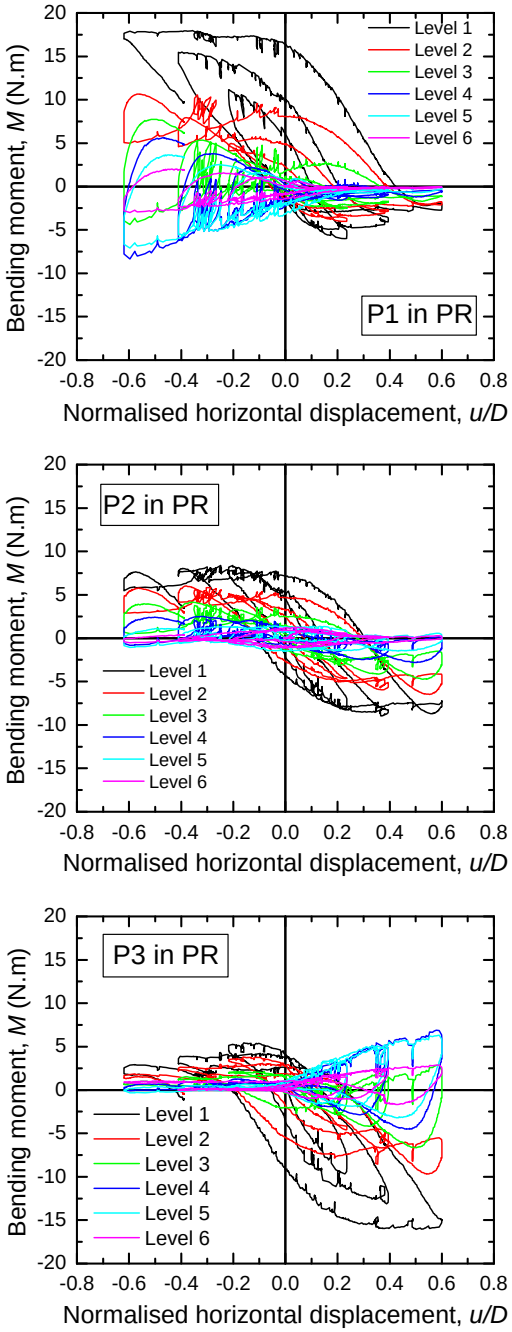

Figure 22 Bending moment on piles node for PR model

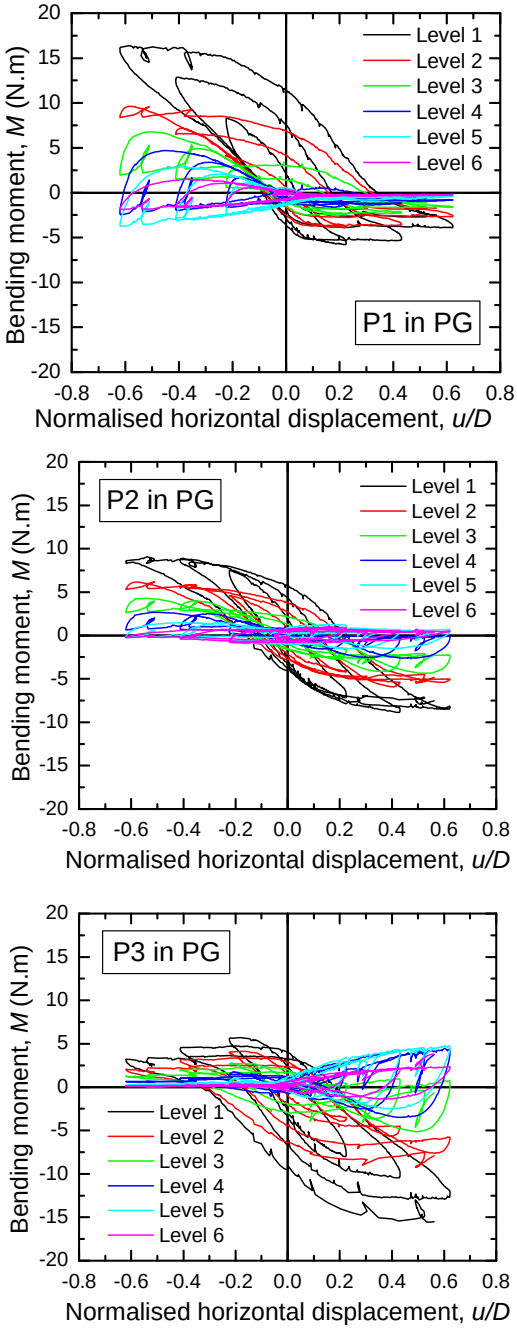

Figure 23 Bending moment on piles node for PG model

The distributions of bending moments, M, along each pile at normalised horizontal displacements, u/D = 0.2, 0.4 and 0.6 are shown in Figures 24 and 25 for PR and PG models, respectively. It is seen that maximum bending moments occur at the top of the piles and that the bending moments of the front piles are much larger than those of the rear piles in both PR and PG models. The bending moments of the centre piles are almost equal in positive and negative loading as expected in both models. For PG case, bending moments are slightly smaller than PR. This means that the horizontal resistance of PR model increases compared with PG without significant bending moment increase at each pile.

Changes of shear forces with u/D at different levels of each pile during horizontal loading are shown in Figures 26 and 27 for PR and PG models, respectively. Similar to the bending moments, the shear forces of the front piles are much larger than those of the rear piles in both PR and PG models. The shear forces of the centre piles are almost equal in positive and negative loading for both models.

If we compare the magnitudes of shear forces of P1 or P3 between PR and PG models, the forces of these piles in PR model are about 1.5 times of those in PG model when the pile is front pile. This result suggests that the piles in PR model are likely to be damaged by shear forces, compared to PG model.

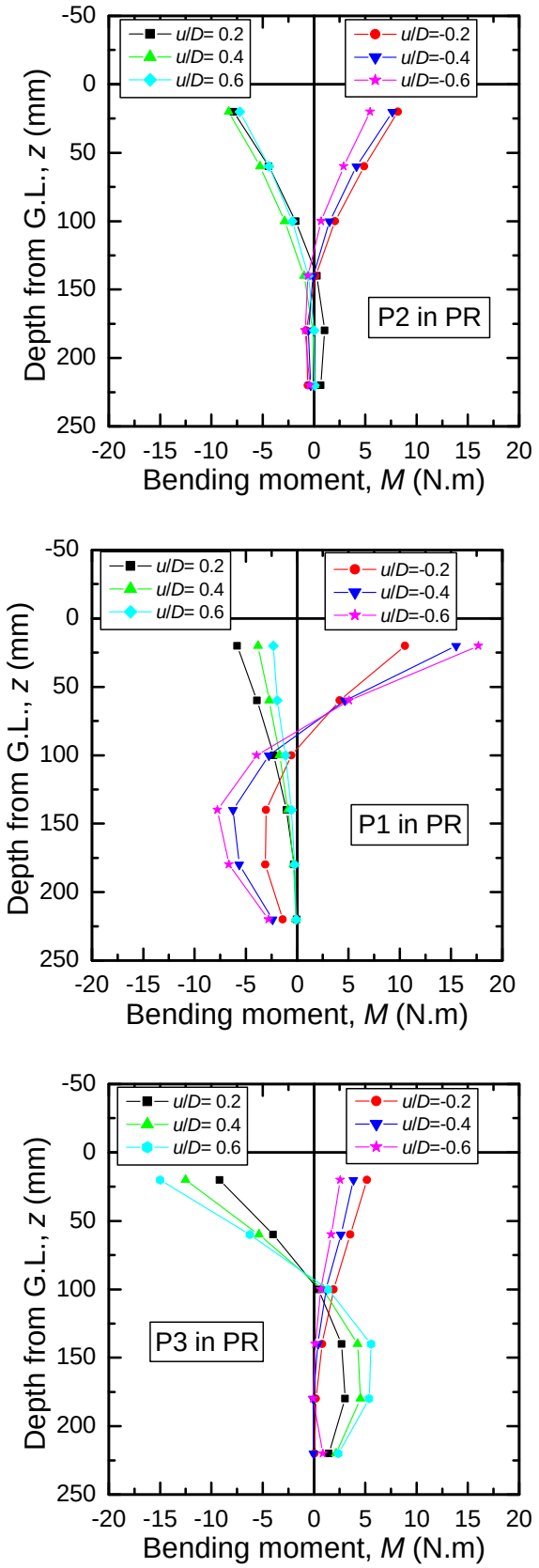

Figure 24 Bending moment distribution of each pile for PR

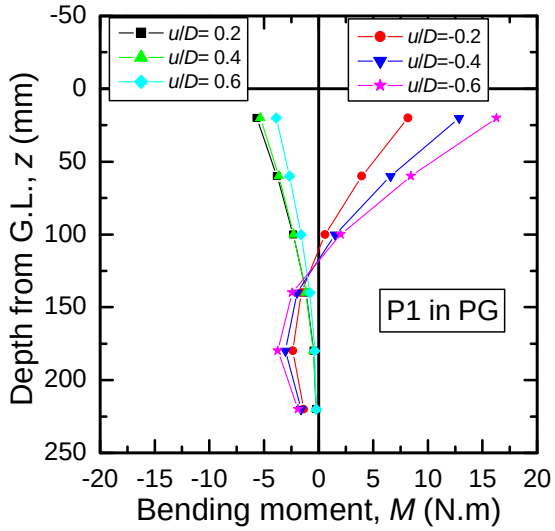

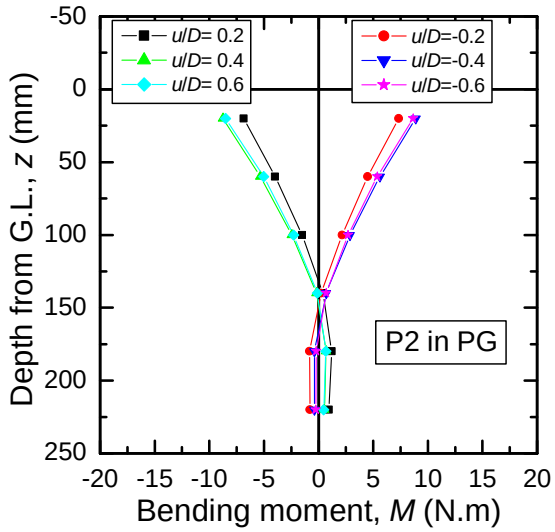

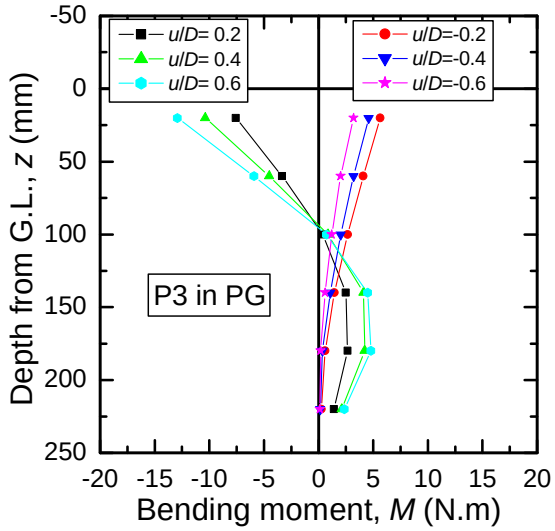

Figure 25 Bending moment distribution of each pile for PG

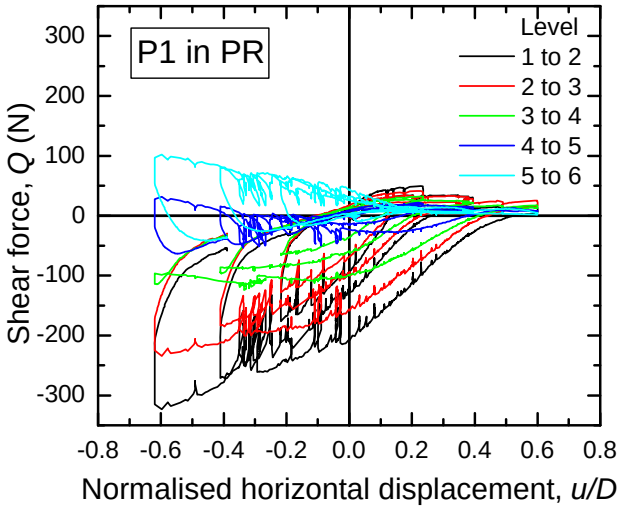

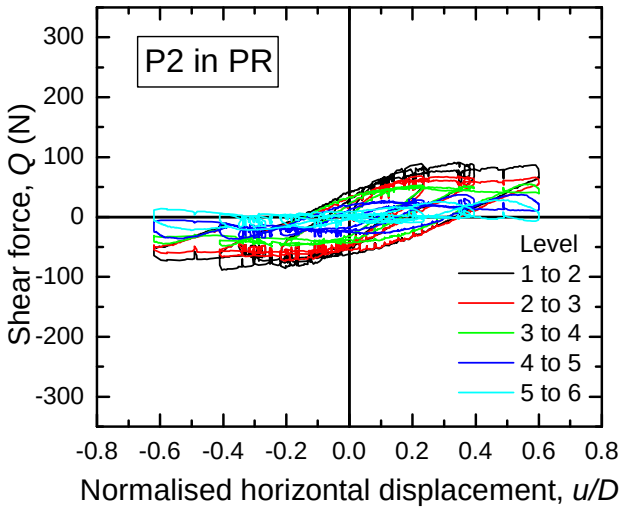

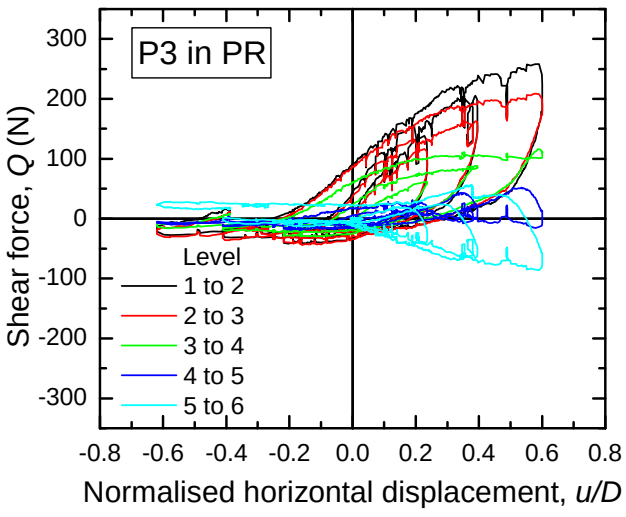

Figure 26 Shear force on piles node for PR

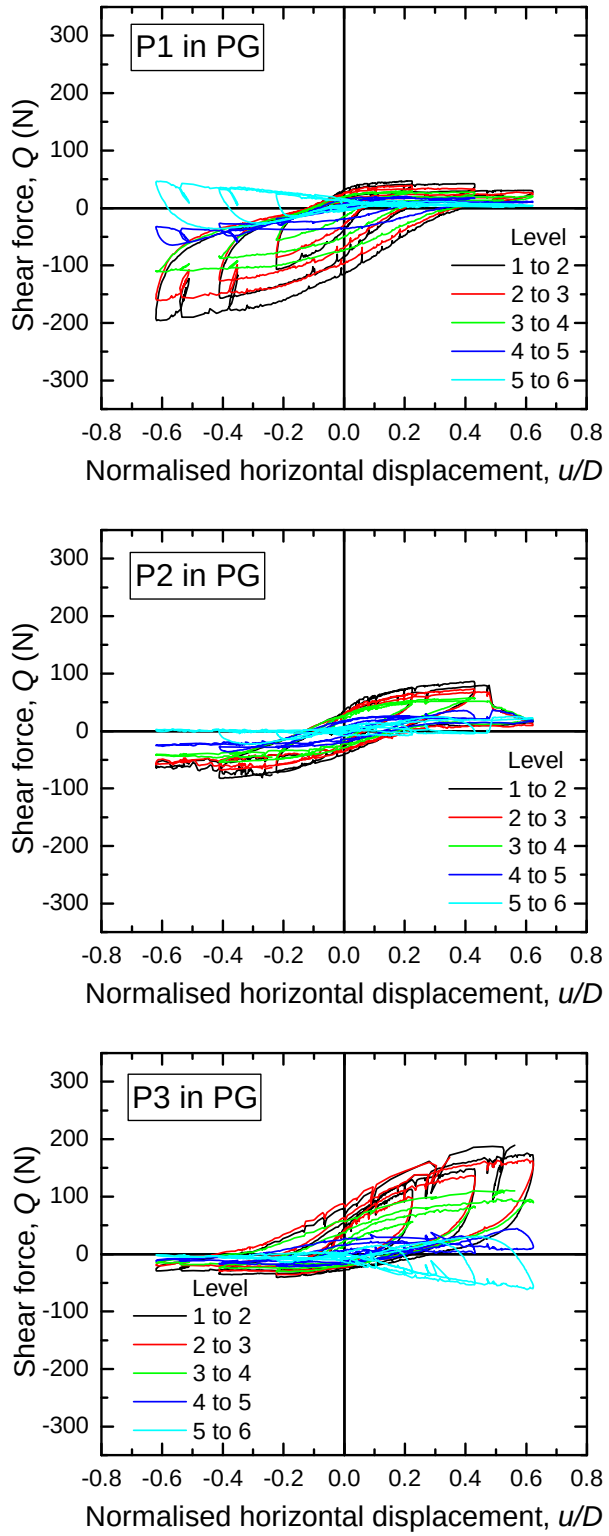

Figure 27 Shear force on piles node for PG

4. CONCLUSIONS

In this study, vertical load tests and cyclic horizontal load tests were carried out on various model foundations (piled and raft alone foundations) in dry sand condition to investigate the response of the foundations. Model piles were friction piles since their tips were not fixed to the bottom of the soil box. In the horizontal load tests, vertical load was applied to the models prior to the start of horizontal loading, in order to take into account the superstructure effect on the foundation behaviour.

Main findings from the experiments and implications for design of piled raft foundations based on the experimental results in this research are as follows:

1) Vertical load test results of capped pile, single pile and small raft showed that, the response of capped pile is not obtained by merely summing the response of small raft and single pile due to the interaction between the raft and the pile. When the response of single pile is compared to the pile component of capped pile, the resistance of the pile in capped pile response is slightly larger than that of the single pile. It may be attributed to the fact that a part of the applied vertical load was transferred to the ground through the raft base, which resulted in an increase of stiffness and strength of the ground and also an increase of horizontal stresses acting on the pile shaft.
2) 3 x single pile, full raft and piled raft responses were examined under vertical loading. The interaction between the piles and the raft could be observed largely in the piled raft than in capped pile-single pile case. Sharing of the applied load between 3 piles and the raft showed that although 3 piles carry most of the load until 0.8 mm settlement of the raft, the raft carries more load than piles after that settlement due to the yielding of piles. Another important point was the axial forces along the centre pile (P2) were larger than those of the edge piles (P1 and P3), which may also explained by transferring the load from the raft to the ground. It may be reasonable to think that the stress level in the soil surrounding P2 is higher than that surrounding P1 and P3.
3) The horizontal loading tests on small raft and full raft showed that, rafts are "horizontal displacement reducers" until slippage occurs. Initial horizontal stiffness, k_h, of both rafts tended to increase as the contact pressure increased. This result also shows the effect of the load transfer from the raft to the ground. Addition to this aspect, a clear size effect of the raft on k_h was observed.
4) The horizontal tests of piled raft and pile group were performed under a constant vertical load. Horizontal resistance of the piled raft was larger than that of the pile group as expected because of the contribution of the raft. In both cases, the front pile carried most of the horizontal load and the rear pile carried least of the horizontal load. The centre pile carried almost the same load both under positive and negative loading. This result may be explained by changes in load transfer from the raft to the soil according to pile positions as well as a conventional concept of interaction among the structure members through the soil.
5) The settlement of the piled raft was a half of the pile group settlement, which indicates an advantage of the piled raft. For both of the models, inclination of the raft is linearly related with the horizontal displacement, which means the inclination of the raft increased with the increase of the horizontal displacement. The proportion of the horizontal load carried by 3 piles was about 80% of the total load. Proportion of vertical load carried by 3 piles was relatively stable during static cyclic horizontal loading of the piled raft model.
6) Bending moment distributions of each pile in piled raft and pile group under positive and negative loadings indicated that the maximum moments occur at the top of the pile. Larger bending moments were observed along the front pile rather than the rear pile in both piled raft and pile group. In case of centre pile, bending moments and shear loads are equal for both positive and negative loadings. Bending moments of the piles in the piled raft was slightly larger than the piles in the pile group, which indicates that the horizontal loading capacity of the piled raft increases without an increase of bending moments along piles. However shear forces on piled raft piles are 1.5 times larger than the piles of pile group, which indicating the shear forces on piles are more critical than bending moments for piles in piled rafts.

As a future work, numerical analyses will be carried out to compare the experimental results with numerical results in order to understand the phenomena deeply.

5. REFERENCES

Horikoshi, K., Matsumoto, T., Hashizume, Y., Watanabe, T., and Fukuyama, H. (2003a) "Performance of piled raft foundations subjected to static vertical and horizontal loads". Int. Journal of Physical Modelling in Geotechnics, 3(2), pp37-50.

Horikoshi, K., Matsumoto, T., Hashizume, Y., and Watanabe, T. (2003b) "Performance of piled raft foundations subjected to dynamic loading". Int. Journal of Physical Modelling in Geotechnics, 3(2), pp51-62.

Iai, S. (1989) "Similitude for shaking table tests on soil-structure-fluid model in 1g gravitational field". Soils and Foundations, 29(1), pp105-118.

Ishizaki, S., Tokimatsu, K., and Nagao, T. (2012) "Overview of semi-rigid pile head connection methods and their erect on buildings in liquefiable soil". Proc. of Testing and Design Methods for Deep Foundations: IS-Kanazawa 2012, Kanazawa, pp13-24.

Matsumoto, T., Fukumura, K., Pastsakorn, K., Horikoshi, K., and Oki, A. (2004a) "Experimental and analytical study on behaviour of model piled rafts in sand subjected to horizontal and moment loading". Int. Journal of Physical Modelling in Geotechnics, 4(3), pp1-19.

Matsumoto, T., Fukumura, K., Oki, A., and Horikoshi, K. (2004b). "Shaking table tests on model piled rafts in sand considering influence of superstructures". Int. Journal of Physical Modelling in Geotechnics, 4(3), pp20-37,

Matsumoto, T., Nemoto, H., Mikami, H., Yaegashi, K., Arai, T. and Kitiyodom, P. (2010) "Load tests of piled raft models with different pile head connection conditions and their analyses". Soils and Foundations, 50(1), pp63-81.

Murono, T., Nishumura, A., and Nagazuma, M. (1997). "Model test on a group-pile considering the vibration of ground in seismic evaluation". Proc. of the 24th Symp. of Japan Earthquake Engrg., pp625-628.

Shibata, T., Yashima, A., and Kimura, M. (1989) "Model tests and analyses of laterally loaded pile groups". Soils and Foundations, 29(1), pp31-44.

Tokimatsu, K., and Suzuki, H. (2004) "Pore water pressure response around piles and its effects on *p-y* behavior during soil liquefaction". Soils and Foundations, 44(6), pp101-110.

Tokimatsu, K., Suzuki, H., and Sato, M. (2005) "Effects of inertial and kinematic interaction on seismic behavior of pile with embedded foundation". Soil Dynamics and Earthquake Engineering, 25(7-10), pp753-762.

Unsever, Y.S., Kawamori, M., Matsumoto, T., and Shimono, S. (2013) "Cyclic horizontal load tests of single pile, pile group and piled raft in model dry sand", Proc. of 18th Southeast Asian Geotechnical & Inaugural AGSSEA Conference, Singapore, pp891-896.

Yamashita, K., Hamada, J., and Yamada, T. (2011) "Field measurements on piled rafts with grid-form deep mixing walls on soft ground ". Geotechnical Engineering Journal of the SEAGS & AGSSEA, 42(2), pp1-10.

Yamashita, K. (2012) "Field measurements on piled raft foundations in Japan". Proc. of Testing and Design Methods for Deep Foundations: IS-Kanazawa 2012, Kanazawa, pp79-96.